Amphiphilic Peptoid-Directed Assembly of Oligoanilines into Highly Crystalline Conducting Nanotubes

Zhiliang Li, Duyen K. Tran, Mary Nguyen, Tengyue Jian, Feng Yan, Samson A. Jenekhe, and Chun-Long Chen**

Dr. Zhiliang Li, Dr. Tengyue Jian, Dr. Feng Yan, Prof. Chun-Long Chen
Physical Sciences Division, Physical and Computational Sciences Directorate
Pacific Northwest National Laboratory
Richland, Washington 99352, United States
E-mail: chunlong.chen@pnnl.gov

Duyen K. Tran, Mary Nguyen, Prof. Samson A. Jenekhe
Department of Chemical Engineering and Department of Chemistry
University of Washington
Seattle, Washington 98195-1750, United States

E-mail: jenekhe@u.washington.edu

Keywords: oligoaniline-peptoid triblocks, molecular self-assembly, crystalline nanotubes, conducting nanotubes, conjugated oligomer-peptoid assembly, oligoaniline nanotubes

Abstract: We report herein the synthesis of a novel amphiphilic diblock peptoid bearing a terminal conjugated oligoaniline and its self-assembly into small-diameter (D ~ 35 nm) crystalline nanotubes with high aspect ratios (> 30). It is shown that both tetraaniline (TANI)-peptoid and bianiline (BANI)-peptoid triblock molecules self-assemble in solution to form rugged highly crystalline nanotubes that are very stable to protonic acid doping and de-doping processes. The similarity of the crystalline tubular structure of the nanotube assemblies revealed by electron microscopy imaging and X-ray diffraction analysis of the nanotube assemblies of TANI-functionalized peptoids and non-functionalized peptoids showed that the peptoid is an efficient ordered structure directing motif for conjugated oligomers. Films of doped TANI-peptoid nanotubes had a dc conductivity of ca. 95 mS/cm

while the thin films of doped un-assembled TANI-peptoids showed a factor of 5.6 lower conductivity, demonstrating impact of the favorable crystalline ordering of the assemblies on electrical transport. These results demonstrate that peptoid-directed supramolecular assembly of tethered π-conjugated oligo(aniline) exemplify a novel general strategy for creating rugged ordered and complex nanostructures that have useful electronic and optoelectronic properties.

1. Introduction

Rapid advances in nanoscience and nanotechnology in recent years have led to immense interests in the molecular engineering of well-defined and functional organic nanomaterials and nanostructures.[1] Nanostructured organic materials have found applications in various fields including energy conversion,[1a, 2] energy storage,[3] field-effect transistors,[2a, 4] biosensors,[1a, 5] and optoelectronics.[1a, 2b, 6] The facile control of the assembly and dimensionality[1a] of such nanostructured materials and the tuning of their diverse physical properties such as charge carrier mobility,[7] catalytic activity,[8] luminescence,[7, 9] electrical conductivity,[10] and electrochemical redox states[1c, 11] by molecular design are of great interest. Molecular self-assembly has been proven to be a promising and facile strategy to access complex yet highly ordered nanostructures with improved or novel properties.[1a, 1b] Furthermore, ease in the synthesis and precise control over the molecular structures of the building blocks can make the assembly more facile while enabling diverse functions in the resulting nanostructures and their potential applications.[1a-d]

Sequence-defined peptoids (poly- or oligo-N-substituted glycines) as a class of synthetic proteinomimetics combine the advantages of both synthetic and biological molecules and have thus been extensively investigated as building blocks for bio-inspired crystalline nanomaterials.[12] We have previously demonstrated that various hierarchically-structured crystalline nanomaterials were obtained by precisely tuning the side chains of amphiphilic diblock peptoids.[13] We have also showed that these peptoid-based nanomaterials are highly tunable and can enable the incorporation of a

wide range of functional groups as sidechains on the peptoid without disrupting the final assembled nanostructures.[13b, 13d] As a result, peptoids have been covalently linked to various classes of materials to generate a wide range of hybrid nanomaterials with novel properties.[13d, 14] However, there are very few studies on the combination of peptoids and π-conjugated organic molecules; prior work mostly focused on the conjugation of porphyrin and helical peptoids to study electron and energy transfer.[15]

π-Conjugated oligomers and polymers have been widely used as semiconducting or functional active materials to fabricate efficient electronic and optoelectronic devices.[2-4, 7, 16] Among them, oligoanilines, especially tetra(aniline) (TANI),[17] which has interesting acid/base- and redox-switchable properties associated with the transition between a conductive salt state and insulating base state,[10a, 18] have been used to assemble nanostructures with increasing dimensionality of 0D micelles and vesicles,[19] 1D nanowires and nanofibers,[10, 17c, 17d, 20] 2D nanoribbons and nanosheets,[17c, 17d] and 3D nanoplates.[17c, 17d] We note that composites of oligo(aniline) and carbon nanotubes[21] as well as oligoanilines covalently linked onto the walls of carbon nanotubes have been reported.[22] Additionally, studies of polyaniline (PANI) nanotubes made by templated synthesis such as using multiwalled carbon nanotubes[23], aluminum oxide membrane[24], or MnO_2 nanotubes[25] have been reported for energy storage applications; however, the PANI nanotubes sizes would be constrained by the size of the initial templates. Template-free synthesis of PANI nanotubes in the presence of various acid dopants[26] have also been reported where the diameters (D) of the PANI nanotubes can be tuned by varying the size of acid dopants. In particular, the outer diameters of these PANI nanotubes vary between 70 – 650 nm while their inner diameters span 15 – 80 nm range.[26] It is important to note that as the outer diameter decreases below 70 nm, the hollow PANI

nanotubes are likely to become solid nanofibers.[26b] Thus, molecular engineering of short oligo(anilines) (N < 10) into crystalline nanotubes at short length scale (D < 50 nm) remains a challenging task that has yet to be explored. We envision that realization of oligoaniline nanotubes could enable simultaneous electronic charge transport within the walls and ion transport inside the hollow tubes, which is highly desirable for applications in many areas including bioelectronics and biosensors,[5, 22] thermoelectric devices,[27] and energy storage devices.[3]

Herein we report the synthesis of novel hybrid materials comprised of covalently linked π-conjugated oligoaniline and sequence-defined diblock peptoid as well as the self-assembly of such hybrid TANI-peptoid triblock molecules into crystalline nanotubes with high aspect ratio featuring tube length spanning over several micrometers while ensuring tube outer diameter at 35 nm. The hybrid TANI-peptoid triblock molecules were found to exhibit acid/base switchable doping and dedoping properties both in the unassembled state and the assembled nanotubes. Thin films of the doped crystalline nanotubes were found to have enhanced conductivity compared to the doped thin films of the un-assembled TANI-peptoid materials. Furthermore, the assembled nanotubes showed excellent stability upon acid doping and base dedoping, demonstrating their great potential for applications requiring robust switching of states of the nanomaterials. Since peptoid-based crystalline nanomaterials are highly stable and exhibit programmable compositions and controllable morphologies, we expect the present strategy of utilizing self-assembling peptoids to precisely organize functional molecules in a long-range order will offer new opportunities in the development of electronic or conducting nanomaterials.

2. Results and Discussion

2.1 Design and Synthesis of Oligoaniline-peptoid Hybrids. Our previous work demonstrated that amphiphilic diblock peptoids containing six polar residues, N-(2-carboxyethyl)glycine (Nce) and six nonpolar residues, N-[2-(4-bromophenyl)ethyl]glycines (*NBrpm*), are able to self-assemble into well-defined crystalline nanotubes.[13d] The molecular structure of this diblock peptoid was found to be highly tunable without disrupting the final assembled tubular nanostructure, for example, various functional groups could be attached to the N-terminus of the backbone. This has inspired our goal here to explore using the tube-forming peptoids as a general platform for directing the assembly of π-conjugated oligomers into novel highly crystalline nanostructures, which could have tunable electronic and optoelectronic properties for applications in many areas. We selected oligoanilines as the π-conjugated oligomer building blocks to test the feasibility of realizing this goal.

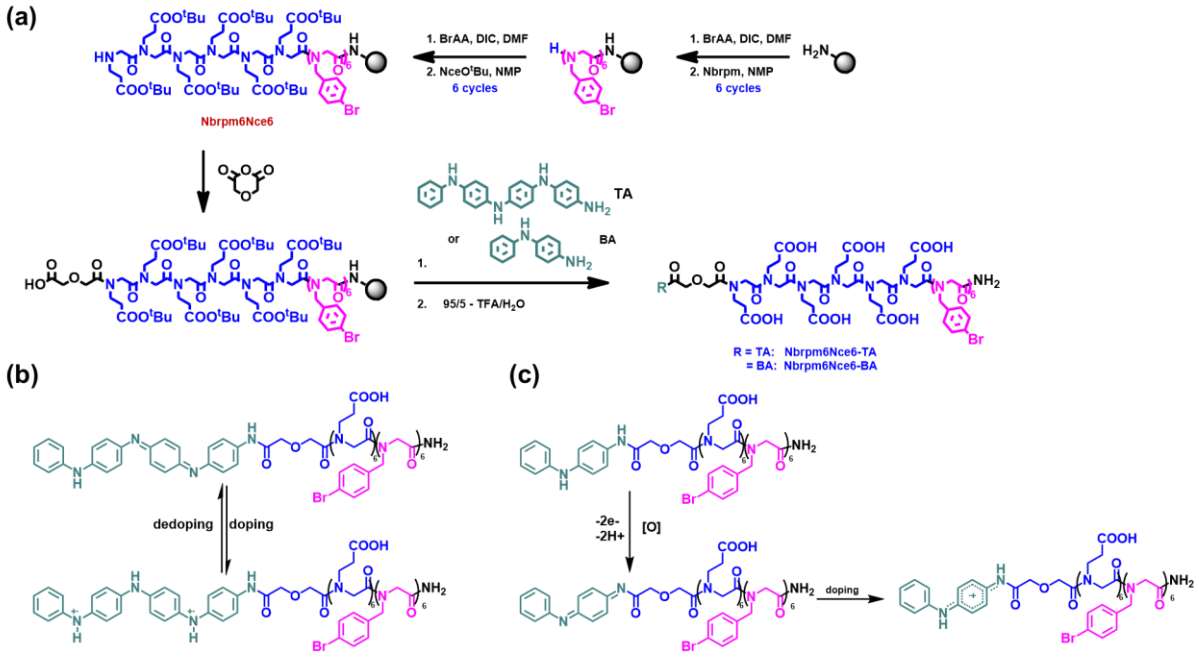

Figure 1. (a) Synthetic route of the TANI-peptoid and BANI-peptoid triblock molecules. (b) Molecular structures of TANI-peptoid upon acid doping and dedoping. (c) Molecular structures of BANI-peptoid upon oxidation in air and acid doping.

The synthesis of the hybrid oligoaniline-peptoid triblock molecules is outlined in **Figure 1**. The target diblock peptoids were synthesized on the solid support using a well-developed sequential monomer addition synthetic approach.[13d] The resin-linked diblock peptoid *Nbrpm6Nce6* (Figure 1a) was further used to react with diglycolic anhydride via ring-opening reaction, which facilitates the acylation reaction on the N-terminus and forms the -COOH end group for coupling with TANI or bianiline (BANI) to make the TANI-peptoid or BANI-peptoid triblock molecules. The final acylation reaction step was conducted overnight at room temperature with shaking to increase the yields. The BANI-peptoid triblock molecule was synthesized to examine the impact of the size of the π-

conjugated oligomer block on the self-assembly of the hybrid materials. The molecular structures, molar mass values, and purity of the peptoids and oligoaniline-peptoids hybrids were established by ultra-performance liquid chromatography-mass spectrometry (UPLC-MS) as is common for peptoids and peptides.[13d] The observed UPLC-MS molecular mass values matched well with the theoretical values (**Figure S1 and S2**), which confirmed the molecular structures of the present oligoaniline-peptoid materials.

The switchable emeraldine base (EB) and emeraldine salt (ES) states of oligo(aniline)-based materials upon protonation and deprotonation of quinoid N atoms by acid or base, make them appealing as model systems in developing peptoid-directed assembly of new electroactive materials. Through doping, the anionic counterion from the dopant is also included in the ES state oligo(aniline)-based materials, which enables the selection of the acid to customize the self-assembled structures.[10a, 17c, 28] The as-synthesized TANI-peptoids were found to be in the emeraldine salt (ES) state due to the use of TFA to cleave the peptoids from resin (Figure 1a). The ES state of the as-made TANI-peptoids could also be inferred from their bright green color, which is associated with formation of polarons, and their limited solubility in non-polar organic solvents (such as chlorobenzene, tetrahydrofuran, etc.) but good solubility in polar solvents like acetonitrile, DMF, and mixtures of H_2O and acetonitrile. We characterized the optical absorption spectra of the EB and ES states of BANI-peptoids and TANI-peptoids in water since both the BANI-peptoids and TANI-

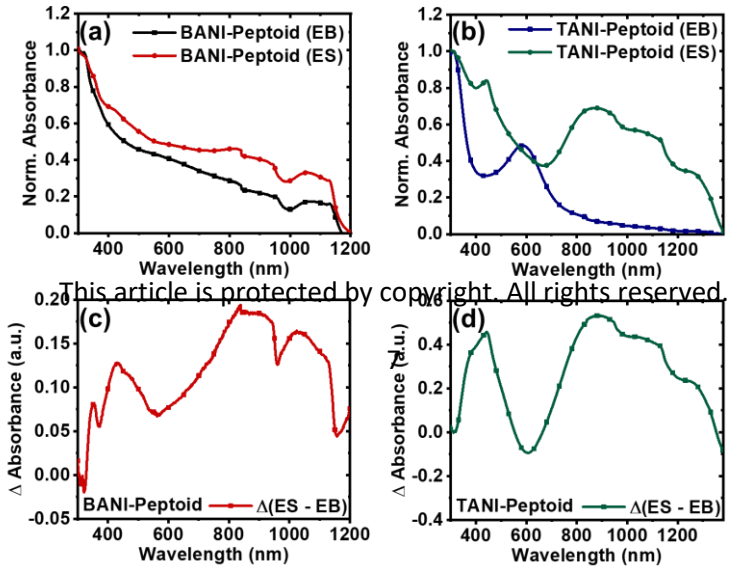

peptoids had good solubility in both EB and ES forms.

Figure 2. (a) Aqueous solution UV-Vis-NIR absorption spectra of BANI-peptoid nanotubes in emeraldine base (EB) state and emeraldine salt (ES) state, (b) Aqueous solution UV-Vis-NIR absorption spectra of TANI-peptoid nanotubes in EB state and ES state, (c) Differential UV-Vis-NIR spectrum of BANI-Peptoid nanotubescalculated by subtracting the spectrum of the EB state from the ES state, and (d) Differential UV-Vis-NIR spectrum of TANI-Peptoid nanotubes calculated by subtracting the spectrum of the EB state from the ES state.

The evolution of optical properties and the nature of charged species in the protonated oligoaniline-peptoid molecules were investigated by obtaining the solution UV-Vis-NIR optical absorption spectra of BANI-peptoid and TANI-peptoid in their emeraldine base (EB) and emeraldine salt (ES) states, which are shown in **Figure 2a and 2b**, respectively. We note that the transition from EB to ES states for both the BANI-peptoid and the TANI-peptoid was achieved by doping with *p*-toluenesulfonic acid, which protonates the imine nitrogen sites. The differential absorption spectra obtained by subtracting the spectrum of EB state from that of ES state are also included in **Figure 2c and 2d**. The undoped BANI-peptoid nanotubes exhibited an absorption peak centered at around 320 nm (~ 3.9 eV), which corresponds to the π-π^* transition of the aniline dimer (Figure 2a), with an extremely broad absorption tail extending into the near IR. These results suggest that the BANI blocks in the hybrid molecules exist in the fully oxidized form (Figure 1c) due to oxygen and water in air.[11] The undoped TANI-peptoid nanotubes showed two distinct absorption peaks at 310 nm (~ 4.0 eV) and 588 nm (~ 2.1 eV) (Figure 2b), corresponding respectively to the π-π^* transition and the intramolecular charge transfer (ICT) from the benzenoid rings to quinoid rings, in good agreement with previous reports of absorption spectra for other oligo(aniline)s and polyaniline.[10a, 17e, 29]

The protonated states of both BANI-peptoid and TANI-peptoid showed very similar absorption features with the π-π^* transition bands at 310 – 320 nm (~ 4 eV) preserved (Figure 2a

and 2b). From the differential absorption spectra (Figure 2c and 2d), two new absorption bands centered at 433 – 441 nm (~ 2.8 – 2.9 eV) and at 840 – 858 nm (~ 1.4 – 1.5 eV) concurrently emerged upon protonating the BANI-peptoid and TANI-peptoid nanotubes. The weaker absorbance changes in BANI-peptoid compared to TANI-peptoid suggest incomplete conversion of BANI-peptoid to the ES state.[30] Both protonated samples also exhibited photobleaching at around 564 – 600 nm (~ 2.0 – 2.2 eV). We note that the abrupt decrease in absorbance at 1180 – 1400 nm can be explained by the relatively localized charge carriers typically observed in oligomers.[17e, 31] These observed changes in the optical absorption spectra of protonated BANI-peptoid and TANI-peptoid collectively suggest that the charged species in the doped samples are positive polarons[11, 32] although the positive polarons found in BANI-peptoid are likely to be more unstable compared to those of TANI. In particular, both nitrogen atoms of the BANI unit are protonated upon doping leading to the polaron structures as presented in Figure 1c. The much shorter chain length of BANI rendered the structure of the positive polarons highly unstable with minimal polaron delocalization. We also found the critical micelle concentration (CMC) of TANI-peptoids to be 0.028 mM (**Figure S3**).

We note that zwitterionic structures are unlikely to be observed in these amphiphilic hybrid materials, BANI-peptoid and TANI-peptoid. During the doping procedure, the environment surrounding the conjugated peptoids is highly acidic; thus, the carboxylic groups (-COOH) in the N-(2-carboxyethyl)glycine block will not be deprotonated to their anionic states ($-COO^-$). Therefore, despite the close spatial arrangement and availability, zwitterionic structures are less likely to be observed in these hybrid materials.

2.2 Self-Assembly of Oligoaniline-peptoid Hybrids. The TANI-peptoid and BANI-peptoid materials were respectively dissolved in water/acetonitrile mixed solvents (v/v = 1:1, 5.0 mM) to obtain clear

solutions, which were placed in a 4 °C refrigerator to facilitate self-assembly using the solvent-evaporation-induced crystallization approach previously developed.[13d] Green precipitates started appearing in 1 day and large number of precipitates were formed by 2 days. The precipitates were sonicated in water to obtain dispersed nanotubes for atomic force microscopy (AFM), transmission electron microscopy (TEM), scanning electron microscopy (SEM) characterizations, and the measurement of electrical conductivity.

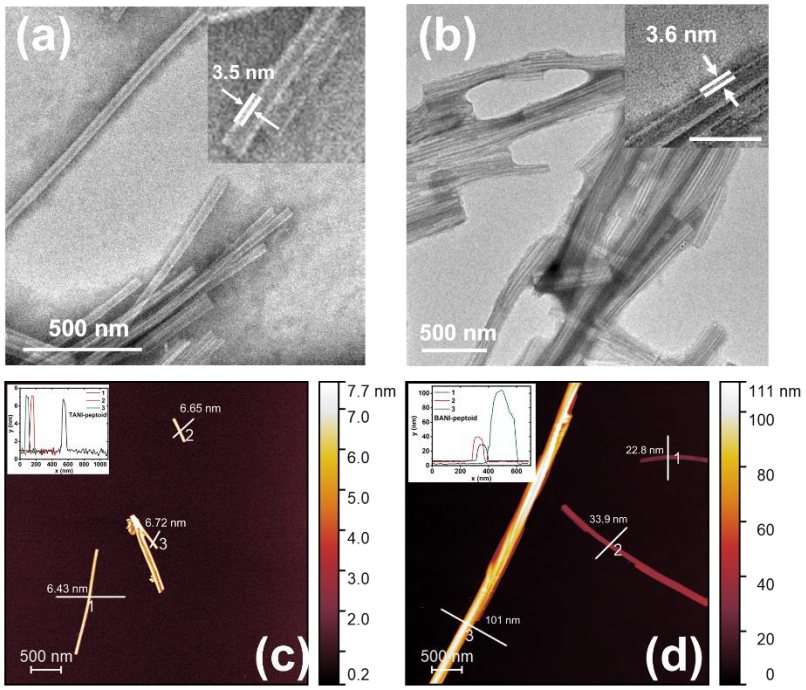

Figure 3. (a and b) TEM images of the nanotubes assembled from TANI-peptoids (a) and BANI-peptoid (b). (c and d) AFM height images of the nanotubes assembled from TANI-peptoids (c) BANI-peptoids (d).

TEM images of the negatively stained samples showed that TANI-peptoid and BANI-peptoid both formed uniform nanotubes (**Figure 3a and 3b**) with diameter and length similar to what we

have reported previously for the un-functionalized diblock peptoids.[13d] *Ex-situ* AFM imaging (**Figure 3c and 3d**) was used to further confirm the self-assembly of both BANI-peptoid and TANI-peptoid. The doped and dedoped TANI-peptoid nanotubes have an average height of about 6.7 nm (Figure 3c and S4), in agreement with other peptoid nanotubes previously reported.[13d] The BANI-peptoid nanotubes showed varying height 22 – 100 nm (Figure 3d). This significant difference in the observed height between TANI-peptoid and BANI-peptoid nanotubes suggest that while the TANI-peptoid nanotubes were isolated as a single nanotube under dry conditions, the BANI-peptoid nanotubes were likely to be a bundle of 5-6 nanotubes (Figure 3b and 3d). Both AFM and TEM results showed that the assembled nanotubes have lengths of over several micrometers; thus, confirming that both TANI-peptoid and BANI-peptoid can be assembled into small-diameter (D ~ 35nm) nanotubes with high aspect ratios (L/D > 30-50). *In-situ* AFM imaging in aqueous solutions of *para*-toluenesulfonic acid was also performed to ensure the stability of these nanotubes in low pH environment. As shown in **Figure S5**, bundles of nanotubes were observed in both height and phase images for both BANI-peptoid and TANI-peptoid. The SEM images (**Figure S6**) of drop-casted films of TANI-peptoids also showed bundles of nanotubes. The high stability these nanotubes upon protonic doping and de-doping was further corroborated by TEM imaging showing the dedoped TANI-peptoids nanotubes retaining their tubular structures (**Figure S7**). These observations confirmed the high stability of the self-assembled nanotubes.

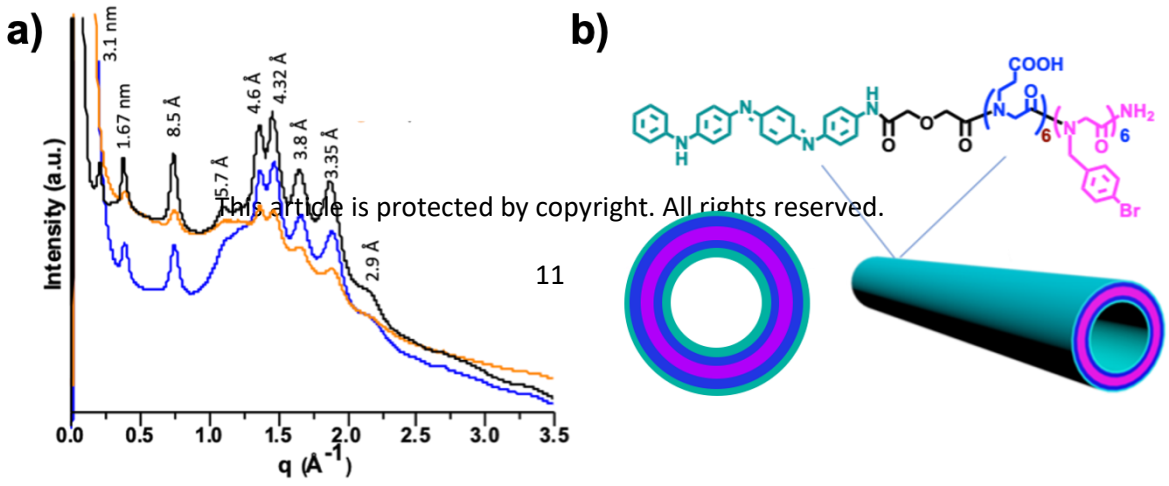

Figure 4. (a) XRD spectra of *Nbrpm6Nce6* (black), BANI-peptoid (blue) and TANI-peptoid (orange). The value above each peak is calculated according to the formula of d = 2π/q. (b) A proposed model showing the molecular packing of the TANI-peptoid nanotube structure: hydrophobic domains are highlighted in pink; polar domains are in blue and TANI tails are in green.

We performed synchrotron-based X-ray diffraction (XRD) to investigate the morphology and detailed structure of the self-assembled nanotubes. The XRD data demonstrate that these nanotubes assembled from oligoaniline-peptoids are highly crystalline (**Figure 4a**) and that they have similar core structures to those assembled from peptoids without TANI or BANI.[13d] The peak at 1.67 nm is assigned to the spacing between two peptoid backbones in the direction with *Nbrpm* groups that are stacked face-to-face. The peak at 5.7 Å is ascribed to the ordered packing of aromatic side chains within the hydrophobic segments. The peak at q = 1.36 $Å^{-1}$ is from the alignment of peptoid chains, which leads to a spacing of 4.6 Å between peptoids. Based on the XRD results, we propose the structure of TANI-peptoid nanotubes shown in Figure 4b, the TANI-peptoid nanotubes have the same core structure as those we reported previously.[13d] The TANI blocks are positioned on the outer and inner surfaces (green color in Figure 4b) of the nanotubes.

2.3 Conductivity of Films of Unassembled TANI-Peptoids and Assembled Nanotubes. We investigated the dc conductivity of films of TANI-peptoid materials in the doped un-assembled form as well as in the doped assembled nanotubes. Films of the un-assembled TANI-peptoid molecules and films of the TANI-peptoid nanotubes were prepared by drop-casting the dispersion of onto glass substrates. *Para*-toluenesulfonic acid (p-TSA) was used as the acid dopant since polyaniline (PANI) doped with p-TSA has been showed to have better conductivity than other acid dopants including

hydrochloric acid (HCl), camphorsulfonic acid (CSA), acetic acid (CH_3COOH), β-naphthalenesulfonic acid (β-NSA), and dodecylbenzene sulfonic acid (DBSA).[33] The higher conductivity obtained from p-TSA doped PANI was attributed to the enhanced charge carrier mobility originating from the highly order interchain packing facilitated by the p-toluenesulfonate anions.[33b] Moreover, p-TSA doped PANI was found to exhibit an order of magnitude greater density of states at the Fermi energy compared to doped PANI bearing other counterions.[34] The mechanism of protonic acid doping of oligoaniline has been studied extensively and established to involve the transition of oligoaniline from its insulating EB state to the conductive ES state.[18b] The dc-conductivity (σ_{dc}) of un-assembled and assembled TANI-peptoid was measured at room temperature by using a 4-point probe. For the un-assembled TANI-peptoids, the dopant to host molar ratio (n_{dopant}:n_{host}) was varied from 2:1 to 75:1 to determine the optimal doping ratio. The average dc-conductivity of TANI-peptoid thin films varied from less than 10^{-5} S/cm at the lowest dopant concentration to (17.0 ± 7.6) x 10^{-3} S/cm at the highest dopant concentration (Table S1). The maximum σ_{dc} of p-TSA doped TANI-peptoid of 2.9 x 10^{-2} S/cm was obtained at the highest dopant concentration. The observed conductivity of doped TANI-peptoid is in good agreement with previous reports on doped bulk tetra(aniline).[10b, 19a, 35]

We investigated the conductivity of doped TANI-peptoid nanotubes at the highest dopant concentration where the highest σ_{dc} of the un-assembled TANI-peptoid was observed. Compared to the un-assembled TANI-peptoid films which were amorphous, the assembled crystalline TANI-peptoid nanotubes showed a nearly 5-fold enhanced conductivity with an average of (9.5 ± 6.4) x 10^{-2} S/cm and a maximum of 0.21 S/cm. We note that the thin-film conductivity fluctuated and drifted significantly during measurements; the dc conductivity of the doped TANI-peptoid nanotubes varied over the 10^{-2} – 10^{-1} S/cm range. The observed variation can be attributed to the possible movement

of ions within the hollow nanotubes. Furthermore, given the excess amount of the dopant, it is likely that the conductivity of both the doped un-assembled TANI-peptoid and the doped TANI-peptoid nanotube films is not purely Ohmic; this suggests that the measured σ_{dc} may have electronic and ionic contributions.

We believe that ion conduction is possible due to the strong hygroscopic nature of p-TSA. In this case, films of doped TANI-peptoid nanotubes were found to swell significantly after exposure to ambient atmosphere for a few minutes, suggesting water uptake as a result of the presence of p-TSA. The presence of water and swollen films would facilitate ion conduction in thin films of doped TANI-peptoid nanotubes. Future studies will aim to deconvolute the contributions of electronic and ionic transport to the observed conductivity. A previous study has showed that the pure Ohmic conductivity of isolated nanostructures of tetra(aniline) is around 0.3 – 1.1 S/cm depending on the dimensionality (1D nanowires, 2D nanoribbons, and 3D nanoplates).[17c] Thus, we believe that if one could measure the conductivity of a single TANI-peptoid nanotube, the conductivity would be much higher than observed for our cast films of nanotubes.

Overall, these measurements demonstrate that the highly ordered alignment of TANI groups achieved through the high crystallinity of assembled TANI-peptoid nanotubes results in a significant enhancement in electrical conductivity compared to the un-assembled TANI-peptoid films. Although the observed conductivity of the highly crystalline TANI-peptoid nanotubes may have contributions from both electronic and ionic transport, the enhanced conductivity due to the crystalline assembly is an important demonstration of the general approach of peptoid-directed organization of organic functional materials. Indeed, organic functional nanomaterials capable of mixed electronic and ionic transport *per se* are also of current interest in areas such as bioelectronics and biosensors.[1a, 5, 22]

Crystals of organic semiconductors are well-known to have superior charge transport and conducting properties than their non-crystalline counterparts,[17d] however, the fragility of such crystals can cause huge difficulty in engineering of various nanostructures or in their applications.[36] The robust nature of the high crystalline and conducting assembled TANI-peptoid nanotubes suggest that this assembly motif could be broadly deployed in creating rugged crystalline organic semiconductor nanostructures.

3. Conclusions

Novel triblock molecules comprised of an amphiphilic sequence-defined diblock peptoid and a π-conjugated oligo(aniline) block have been synthesized and demonstrated to self-assemble into highly crystalline conducting nanotubes with small diameter (D ~ 35 nm) and high aspect ratios (L/D > 30). The TANI-peptoid nanotube assemblies were found to be very stable under doping and dedoping processes. AFM, TEM and SEM imaging and X-ray diffraction analysis of the nanotube assemblies of TANI-functionalized peptoids and non-functionalized peptoids showed that the crystalline tubular structure of the assemblies was very similar, demonstrating that the peptoid is the ordered structure directing motif.

Although both oligoaniline-peptoid materials, including the BANI-peptoid and TANI-peptoid, self-assembled into highly crystalline nanotubes, only the un-assembled and assembled TANI-peptoid were electrically conducting when doped, which demonstrates the effect of the π-conjugated oligo(aniline) block size in the charge transport properties of the hybrid materials. Thin films of doped TANI-peptoid nanotubes had an average dc-conductivity of 95 ± 64 mS/cm while the thin films of doped un-assembled TANI-peptoids showed a lower average dc-conductivity of 17 ± 8 mS/cm. The enhancement in electrical transport in TANI-peptoids upon self-assembly can be

understood in terms of the favorable crystalline ordering of the TANI groups in the nanotubes. These results demonstrate that peptoid-directed supramolecular self-assembly of π-conjugated oligo(aniline) exemplify a novel general strategy for creating rugged ordered and complex nanostructures that have useful electronic and optoelectronic properties.

4. Experimental Section/Methods

Materials. β-Alanine t-butyl ester was converted from its hydrochloride salt purchased from Chem-Impex International, Inc. The solution of the hydrochloride salt in CH_2Cl_2 was washed by sodium hydroxide (NaOH) aqueous solution, then concentrated to give β-alanine t-butyl ester. Bromoacetic acid and trifluoroacetic acid (TFA) were purchased from Chem-Impex International, Inc and used as received. 4-Bromobenzylamine was purchased from Oakwood Products, Inc and used as received. N, N-diisopropylethylamine (DIPEA), 4-Dimethylaminopyridine (DMAP) and diglycolic anhydride were purchased from TCI America and used as received. (2-(1H-benzotriazol-1-yl)-1,1,3,3-tetramethyluronium hexafluorophosphate (HBTU) was purchased from Aapptec and used as received. All other reagents were obtained from commercial sources and used without further purification. MilliQ water at 18 MΩ cm was used for all experiments.

Synthesis of Oligo(aniline)-peptoid Hybrids. The synthesis of oligoanilines, tetra(aniline) (TANI) and bianiline (BANI), followed the reported procedures.[1] The resin linked diblock peptoid *Nbrpm6Nce6* (Figure 1) was synthesized using a solid phase submonomer approach as described previously.[2] An acylation reaction was then performed by ring-opening reaction between the N-terminus of *Nbrpm6Nce6* and diglycolic anhydride (0.6 M) in DCM/TEA (v/v = 2/1). The mixture was agitated overnight at room temperature, drained, and washed five times with DMF. Then 1.6 mL of the tetra(aniline) (TANI) or bianiline (BANI) solution (0.6 M) in N-methyl-2-pyrrolidone (NMP), 0.2 mL of

DIPEA, 360 mg of HUBT and 18 mg of DMAP were added into the reaction chamber, followed by agitation overnight at room temperature.[3] The solution was drained from the resin, and the resin was washed five times with DMF. Each of the DMF washes consisted of the addition of 1.5 mL of DMF, followed by agitation for 1 min; and this was repeated five times. The final crude product was cleaved from the resin by addition of 2 mL of TFA/water (v/v = 95/5) and agitation for 30 minutes. The dark green solution was collected by filtration, followed by washing the resin with 95% TFA (1 mL, twice). The solvent was then evaporated off under a stream of N_2 gas, yielding the green oily crude product, which was dissolved in H_2O/CH_3CN (v/v = 1:3) for HPLC purification. The crude products were purified by reverse-phase HPLC on a XBridge Prep C18 10 µm Optimum Bed Density (OBD) (10 µm, 19 mm × 100 mm), using adaptable gradient of acetonitrile in H_2O with 0.1% TFA over 15 min. Purified peptoids were analyzed using Waters ACQUITY reverse-phase UPLC (corresponding gradient at 0.4 mL/min over 7 min at 40 °C with a ACQUITYBEH C18, 1.7 µm, 2.1 mm × 50 mm column) that was connected with a Waters SQD2 mass spectrometry system. The purified oligoaniline-peptoid was lyophilized at least twice from its solution in a mixture of water and acetonitrile (v/v = 1:3). The oligoaniline-peptoid powders were finally divided into small portions (1.0 × 10^{-6} mol) and stored at −80 °C.

Self-assembly of Oligo(aniline)-peptoids. The self-assembly of TANI-peptoid followed the well-developed evaporation-induced-crystallization method reported from our previous work.[2] In a small vial, 1.0 µmol of lyophilized TANI-peptoid green powders were dissolved in 200 µL of water and acetonitrile (v/v = 1:1) to make a 5.0 mM of clear solution, which has a pH about 3.0. The vial was then loosely capped and put in 4 °C refrigerator for slow evaporation of the solvents. About 2 days

later, green precipitates composed of a large number of nanotubes were obtained. The mixture was sonicated to get the dispersed nanotubes in water before doing measurements.

Optical Absorption Characterizations. UV-Vis-NIR absorption spectra were measured on a PerkinElmer model Lambda 900 UV-Vis/near-IR spectrophotometer. Absorption spectra of the solutions were recorded at a concentration of 100 µM in quartz cuvette with 1cm path length. Solution absorption spectra of *doped* TANI-peptoid and BANI-peptoid were obtained by solubilizing TANI-peptoid and BANI-peptoid in aqueous solution of *para*-toluene sulfonic acid. (*p*-TSA). Both the *p*-TSA doped TANI-peptoid and BANI-peptoid solutions showed green colors. The *de-doped* TANI-peptoid and BANI-peptoid were prepared by solubilizing them in aqueous potassium hydroxide (KOH) solution. Both solutions exhibited light blue/purple colors.

Fabrication and doping of TANI-peptoid thin films. In the case of the ***un-assembled*** material, 0.1 µmol TANI-peptoid was dissolved in N-Methyl-2-Pyrrolidone (NMP) at a concentration of 5 mM and sonicated to ensure complete dissolution. The acid dopant, *para*-toluenesulfonic acid (*p*-TSA), was dissolved in NMP at a concentration of 0.1 M. The un-assembled TANI-peptoid and *p*-TSA were mixed at different molar ratios. The blend solutions were then drop-casted onto cleaned glass substrates and dried under vacuum. In the case of the ***assembled*** material, trifluoroacetic acid (TFA) was added dropwise into 1µmol TANI-peptoid in a small vial until the TANI-peptoid was fully dissolved. A steady stream of N_2 gas was flown into the vial to remove the TFA. Once all of the TFA was removed, 200 µL of mixed water and acetonitrile (H_2O:CH_3CN = 1:1 (v:v)) was added into the vial. The solution was placed in the fridge at 4^{o}C for over 2 days to facilitate the self-assembly process. The dopant, *p*-TSA, was dissolved in water at a concentration of 0.1 M and mixed with the

assembled TANI-peptoid at different molar ratios. The blend solutions were then drop-casted onto cleaned glass substrates and dried under vacuum.

Electrical Conductivity. The room temperature dc conductivity of the TANI-peptoid thin films was measured using a colinear 4-point probe instrument (Alessi CPS-06 contact probe station) with a 1.55 mm tip to tip spacing connected to a Keithley 2400 source meter.

Atomic force microscopy (AFM) Imaging. Characterization of the surface morphology of the TANI-peptoid thin films was done by using a Bruker Dimension scanning probe microscope (SPM) system. Thin films of the self-assembled TANI-peptoid were fabricated by drop-casting the aqueous solution containing the TANI-peptoid nanotubes onto either glass or mica substrates and dried in vacuum oven or under Argon gas before characterization.

Transmission electron microscopy (TEM) Imaging. TEM images were collected on a FEI Tecnai instrument operating at an accelerating voltage of 200 keV. The samples for TEM imaging were prepared as follow: 2 µL solution of the assemblies was diluted in 5 µL of deionized water and dropped onto carbon-coated copper grids. The droplets were removed by a piece of filter paper after 10 min. Then, the samples were negatively stained by putting 5 µL of phosphotungstic acid (wt 2% in H_2O) onto the TEM grid for 2 min, followed by removing the extra solution using a piece of filter paper and the samples were then dried in air.

X-ray diffraction analysis (XRD). Powder XRD data were collected at a multiple-wavelength anomalous diffraction and monochromatic macromolecular crystallography beamline, 8.3.1, at the Advanced Light Source located at Lawrence Berkeley National Laboratory. Beamline 8.3.1 has a 5T single pole superbend source with an energy range of 5–17 keV. Data were collected with a 3 × 3

CCD array (ADSC Q315r) detector at a wavelength of 1.1159 Å. Data sets were collected with the detector 200 mm from the sample. Peptoid nanotube suspensions or pellets were pipetted onto a Kapton mesh (MiTeGen) and dried. All XRD Data were processed with custom Python scripts.

Critical Aggregation Concentration. All fluorescence studies were performed on a Fluorescence Spectrophotometer (Tecan Austria GmbH). The parameters including excitation and emission slit widths were set at 20 nm, gain with 80. 10 µL of a 0.5 mg/mL pyrene solution in acetone was added to 900 µL EB TANI-Peptoid solutions in CH_3CN/H_2O (v/v = 1:1) with different concentrations (Figure S3). After shaking for 10 min, the pyrene emission of each solution was obtained by scanning from 360 to 450 nm with excitation wavelength at 337 nm. The CMC was chosen at the concentration where the pyrene exhibited an apparent decrease in the I_{373nm}/I_{383nm} ratio with increasing concentration.

Supporting Information

Supporting Information is available from the Wiley Online Library or from the author.

Acknowledgements

This work was supported by the U.S. Department of Energy, Office of Science, Office of Basic Energy Sciences as part of the Energy Frontier Research Centers program: CSSAS-The Center for the Science of Synthesis Across Scales under award number DE-SC0019288. Pacific Northwest National Laboratory (PNNL) is multi-program national laboratory operated for Department of Energy by Battelle under Contracts No. DE-AC05-76RL01830.

Received: ((will be filled in by the editorial staff))
Revised: ((will be filled in by the editorial staff))
Published online: ((will be filled in by the editorial staff))

References

[1] a) F. S. Kim, G. Ren, S. A. Jenekhe, *Chem. Mater.* **2011**, *23*, 682-732; b) J.-M. Lehn, *Makromolekulare Chemie. Macromolecular Symposia* **1993**, *69*, 1-17; c) R. Xu, L. Du, D. Adekoya, G. Zhang, S. Zhang, S. Sun, Y. Lei, *Adv. Energy Mater.* **2020**, 2001537; d) C. Cui, D. H. Park, D. J. Ahn, *Adv. Mater.* **2020**, 2002213; e) T. W. Kelley, P. F. Baude, C. Gerlach, D. E. Ender, D. Muyres, M. A. Haase, D. E. Vogel, S. D. Theiss, *Chem. Mater.* **2004**, *16*, 4413-4422.

[2] a) P.-T. Wu, H. Xin, F. S. Kim, G. Ren, S. A. Jenekhe, *Macromolecules* **2009**, *42*, 8817-8826; b) G. Ren, E. Ahmed, S. A. Jenekhe, *J. Mater. Chem.* **2012**, *22*, 24373-24379.

[3] J. Wu, X. Rui, C. Wang, W.-B. Pei, R. Lau, Q. Yan, Q. Zhang, *Adv. Energy Mater.* **2015**, *5*, 1402189.

[4] a) A. L. Briseno, S. C. B. Mannsfeld, P. J. Shamberger, F. S. Ohuchi, Z. Bao, S. A. Jenekhe, Y. Xia, *Chem. Mater.* **2008**, *20*, 4712-4719; b) S. G. Hahm, Y. Rho, J. Jung, S. H. Kim, T. Sajoto, F. S. Kim, S. Barlow, C. E. Park, S. A. Jenekhe, S. R. Marder, M. Ree, *Adv. Funct. Mater.* **2013**, *23*, 2060-2071; c) A. L. Briseno, S. C. B. Mannsfeld, X. Lu, Y. Xiong, S. A. Jenekhe, Z. Bao, Y. Xia, *Nano Lett.* **2007**, *7*, 668-675; d) A. L. Briseno, S. C. B. Mannsfeld, C. Reese, J. M. Hancock, Y. Xiong, S. A. Jenekhe, Z. Bao, Y. Xia, *Nano Lett.* **2007**, *7*, 2847-2853.

[5] a) J. Rivnay, R. M. Owens, G. G. Malliaras, *Chem. Mater.* **2014**, *26*, 679-685; b) D. T. Simon, E. O. Gabrielsson, K. Tybrandt, M. Berggren, *Chem. Rev.* **2016**, *116*, 13009-13041; c) B. D. Paulsen, K. Tybrandt, E. Stavrinidou, J. Rivnay, *Nat. Mater.* **2020**, *19*, 13-26.

[6] a) G. Ren, P.-T. Wu, S. A. Jenekhe, *ACS Nano* **2011**, *5*, 376-384; b) H. Xin, O. G. Reid, G. Ren, F. S. Kim, D. S. Ginger, S. A. Jenekhe, *ACS Nano* **2010**, *4*, 1861-1872; c) H. Xin, F. S. Kim, S. A. Jenekhe, *J. Am. Chem. Soc.* **2008**, *130*, 5424-5425.

[7] E. Ahmed, T. Earmme, G. Ren, S. A. Jenekhe, *Chem. Mater.* **2010**, *22*, 5786-5796.

[8] a) Z. Yin, Q. Zheng, *Adv. Energy Mater.* **2012**, *2*, 179-218; b) P. Li, G. Xu, N. Wang, B. Guan, S. Zhu, P. Chen, M. Liu, *Adv. Funct. Mater.* **2021**, 2100367; c) A. L. Briseno, S. C. B. Mannsfeld, E. Formo, Y. Xiong, X. Lu, Z. Bao, S. A. Jenekhe, Y. Xia, *J. Mater. Chem.* **2008**, *18*, 5395-5398; d) Q. Zhou, C. M. Li, J. Li, X. Cui, D. Gervasio, *J. Phys. Chem. C* **2007**, *111*, 11216-11222.

[9] a) A. Nitti, D. Pasini, *Adv. Mater.* **2020**, *32*, 1908021; b) R. Mazzaro, A. Vomiero, *Adv. Energy Mater.* **2018**, *8*, 1801903.

[10] a) O. A. Bell, G. Wu, J. S. Haataja, F. Brommel, N. Fey, A. M. Seddon, R. L. Harniman, R. M. Richardson, O. Ikkala, X. Zhang, C. F. J. Faul, *J. Am. Chem. Soc.* **2015**, *137*, 14288-14294; b) W. Lyu, J. Feng, W. Yan, C. F. J. Faul, *J. Mater. Chem. C* **2015**, *3*, 11945-11952.

[11] B. M. Mills, N. Fey, T. Marszalek, W. Pisula, P. Rannou, C. F. J. Faul, *Chem. Eur. J.* **2016**, *22*, 16950-16956.

[12] a) J. Sun, R. N. Zuckermann, *ACS Nano* **2013**, *7*, 4715-4732; b) N. Gangloff, J. Ulbricht, T. Lorson, H. Schlaad, R. Luxenhofer, *Chem. Rev.* **2016**, *116*, 1753-1802.

[13] a) Y. Song, M. Wang, S. Li, H. Jin, X. Cai, D. Du, H. Li, C.-L. Chen, Y. Lin, *Small* **2018**, *14*, 1803544; b) H. B. Jin, F. Jiao, M. D. Daily, Y. L. Chen, F. Yan, Y. H. Ding, X. Zhang, E. J. Robertson, M. D. Baer, C. L. Chen, *Nat. Commun* **2016**, *7*, 8; c) H. Jin, T. Jian, Y. H. Ding, Y. Chen, P. Mu, L. Wang, C. L. Chen, *Biopolymers* **2019**, *110*, e23258; d) H. Jin, Y.-H. Ding, M. Wang, Y. Song, Z. Liao, C. J. Newcomb, X. Wu, X.-Q. Tang, Z. Li, Y. Lin, F. Yan, T. Jian, P. Mu, C.-L. Chen, *Nat. Commun.* **2018**, *9*, 270.

[14] a) A. S. Knight, E. Y. Zhou, M. B. Francis, R. N. Zuckermann, *Adv. Mater.* **2015**, *27*, 5665-5691; b) A. S. Culf, *Biopolymers* **2019**, *110*, e23285.

[15] a) B. Kang, S. Chung, Y. D. Ahn, J. Lee, J. Seo, *Org. Lett.* **2013**, *15*, 1670-1673; b) B. Kang, W. Yang, S. Lee, S. Mukherjee, J. Forstater, H. Kim, B. Goh, T.-Y. Kim, V. A. Voelz, Y. Pang, J. Seo, *Sci. Rep.* **2017**, *7*, 4786; c) Y. Kim, B. Kang, H.-Y. Ahn, J. Seo, K. T. Nam, *Small* **2017**, *13*, 1700071.

[16] F. J. M. Hoeben, P. Jonkheijm, E. W. Meijer, A. P. H. J. Schenning, *Chem. Rev.* **2005**, *105*, 1491-1546.

[17] a) T. G. Dane, P. T. Cresswell, O. Bikondoa, G. E. Newby, T. Arnold, C. F. J. Faul, W. H. Briscoe, *Soft Matter* **2012**, *8*, 2824-2832; b) W. E. Ford, D. Gao, F. Scholz, G. Nelles, F. von Wrochem, *Chem. Mater.* **2013**, *25*, 3603-3613; c) Y. Wang, H. D. Tran, L. Liao, X. Duan, R. B. Kaner, *J. Am. Chem. Soc.* **2010**, *132*, 10365-10373; d) Y. Wang, J. Liu, H. D. Tran, M. Mecklenburg, X. N. Guan, A. Z. Stieg, B. C. Regan, D. C. Martin, R. B. Kaner, *J. Am. Chem. Soc.* **2012**, *134*, 9251-9262; e) Z. Shao, Z. Yu, J. Hu, S. Chandrasekaran, D. M. Lindsay, Z. Wei, C. F. J. Faul, *J. Mater. Chem.* **2012**, *22*, 16230-16234; f) C. U. Udeh, N. Fey, C. F. J. Faul, *J. Mater. Chem.* **2011**, *21*, 18137-18153.

[18] a) K. Lee, S. Cho, S. Heum Park, A. J. Heeger, C.-W. Lee, S.-H. Lee, *Nature* **2006**, *441*, 65-68; b) C.-W. Lin, R. L. Li, S. Robbennolt, M. T. Yeung, G. Akopov, R. B. Kaner, *Macromolecules* **2017**, *50*, 5892-5897.

[19] a) C. U. Udeh, P. Rannou, B. P. Brown, J. O. Thomas, C. F. J. Faul, *J. Mater. Chem. C* **2013**, *1*, 6428-6437; b) W. Lv, J. Feng, W. Yan, C. F. J. Faul, *J. Mater. Chem. B* **2014**, *2*, 4720-4725; c) H. Kim, S.-M. Jeong, J.-W. Park, *J. Am. Chem. Soc.* **2011**, *133*, 5206-5209; d) H. Kim, T.-G. Kim, J.-W. Park, *Macromol. Res.* **2013**, *21*, 815-820; e) R. Arukula, C. R. K. Rao, R. Narayan, B. Sreedhar, *Polymer* **2015**, *77*, 334-344.

[20] I. Arioz, O. Erol, G. Bakan, F. B. Dikecoglu, A. E. Topal, M. Urel, A. Dana, A. B. Tekinay, M. O. Guler, *ACS Appl. Mater. Interfaces* **2018**, *10*, 308-317.

[21] X. Liu, Y. Zhou, D. Chao, *Macromol. Res.* **2020**, *28*, 721-726.

[22] T.-C. Huang, L.-C. Yeh, H.-Y. Huang, Z.-Y. Nian, Y.-C. Yeh, Y.-C. Chou, J.-M. Yeh, M.-H. Tsai, *Polym. Chem.* **2014**, *5*, 630-637.

[23] W. Feng, X. D. Bai, Y. Q. Lian, J. Liang, X. G. Wang, K. Yoshino, *Carbon* **2003**, *41*, 1551-1557.

[24] F. Cheng, W. Tang, C. Li, J. Chen, H. Liu, P. Shen, S. Dou, *Chem. - Eur. J.* **2006**, *12*, 3082-3088.

[25] W. Chen, R. B. Rakhi, H. N. Alshareef, *J. Mater. Chem. A* **2013**, *1*, 3315-3324.

[26] a) H. Qiu, M. Wan, B. Matthews, L. Dai, *Macromolecules* **2001**, *34*, 675-677; b) Z. Wei, Z. Zhang, M. Wan, *Langmuir* **2002**, *18*, 917-921; c) Z. Zhang, M. Wan, Y. Wei, *Adv. Funct. Mater.* **2006**, *16*, 1100-1104; d) L. Zhang, H. Peng, Z. D. Zujovic, P. A. Kilmartin, J. Travas-Sejdic, *Macromol. Chem. Phys.* **2007**, *208*, 1210-1217; e) L. Zhang, H. Peng, J. Sui, P. A. Kilmartin, J. Travas-Sejdic, *Curr. Appl. Phys.* **2008**, *8*, 312-315.

[27] B. Russ, A. Glaudell, J. J. Urban, M. L. Chabinyc, R. A. Segalman, *Nat. Rev. Mater.* **2016**, *1*, 16050.

[28] a) L. W. Shacklette, J. F. Wolf, S. Gould, R. H. Baughman, *J. Chem. Phys.* **1988**, *88*, 3955-3961; b) J. P. Pouget, M. E. Jozefowicz, A. J. Epstein, X. Tang, A. G. MacDiarmid, *Macromolecules* **1991**, *24*, 779-789; c) Z. Wei, T. Laitinen, B. Smarsly, O. Ikkala, C. F. Faul, *Angew. Chem. Int. Ed.* **2005**, *117*, 761-766.

[29] W. Wang, A. G. MacDiarmid, *Synth. Met.* **2002**, *129*, 199-205.

[30] Y. Cao, P. Smith, A. J. Heeger, *Synth. Met.* **1989**, *32*, 263-281.

[31] B. Pałys, P. Celuch, *Electrochim. Acta* **2006**, *51*, 4115-4124.

[32] a) S. Stafström, J. L. Brédas, A. J. Epstein, H. S. Woo, D. B. Tanner, W. S. Huang, A. G. MacDiarmid, *Phys. Rev. Lett.* **1987**, *59*, 1464-1467; b) A. J. Epstein, J. M. Ginder, F. Zuo, H. S. Woo, D. B. Tanner, A. F. Richter, M. Angelopoulos, W. S. Huang, A. G. MacDiarmid, *Synth. Met.* **1987**, *21*, 63-70; c) Y. H. Kim, C. Foster, J. Chiang, A. J. Heeger, *Synth. Met.* **1988**, *26*, 49-59; d) Y. Cao, *Synth. Met.* **1990**, *35*, 319-332.

[33] a) L. Zhang, M. Wan, Y. Wei, *Macromol. Rapid Commun.* **2006**, *27*, 366-371; b) J. Wu, Y. Sun, W. Xu, Q. Zhang, *Synth. Met.* **2014**, *189*, 177-182; c) D. Poussin, H. Morgan, P. J. Foot, *Polym. Int.* **2003**, *52*, 433-438.

[34] V. I. Krinichnyi, S. V. Tokarev, H. K. Roth, M. Schrodner, B. Wessling, *Synth. Met.* **2006**, *156*, 1368-1377.

[35] Z. Wei, C. F. J. Faul, *Macromol. Rapid Commun.* **2008**, *29*, 280-292.

[36] a) S. Ghosh, C. M. Reddy, *Angew. Chem. Int. Ed.* **2012**, *124*, 10465-10469; b) S. Hayashi, T. Koizumi, *Angew. Chem. Int. Ed.* **2016**, *128*, 2751-2754.

Peptoid-directed supramolecular self-assembly of π-conjugated oligoanilines into highly ordered, crystalline, and conducting nanotubes.